CALCULATED ORGAN EQUIVALENT DOSES FOR INDIVIDUALS IN A SITTING POSTURE ABOVE A CONTAMINATED GROUND AND A PET IMAGING ROOM

Lin Su, Bin Han and X. George Xu*
Nuclear Engineering and Engineering Physics Program, Rensselaer Polytechnic Institute, Troy, NY 12180, USA

*Corresponding author: xug2@rpi.edu

In this paper, phantoms representing sitting postures were developed and implemented in the MCNPX code to perform dose calculations. For the ground contamination case, isotropic planar source of ^{137}Cs was used. The male sitting phantom received an effective dose rate of 37.73 nSv h^{-1} for a contamination of 30 kBq m^{-2}. The gonadal equivalent dose of the male sitting phantom was 40 % larger than that from the standing phantom. For the positron emission tomography clinic, a point photon source with the energy of 511 keV was used. The gonadal equivalent dose of the male sitting phantom was 117 % larger than that for the standing phantom. For an 8-h day, the effective dose of the sitting phantom was 2.54 μSv for 550 MBq F-18. This study concludes that phantoms with realistic postures could and should be considered in organ equivalent dose calculations in certain environmental and medical dosimetry studies where accurate data are desired.

INTRODUCTION

Computational human phantoms have been utilised to assess organ equivalent doses and associated risk. Most existing phantoms were constructed in a standing position with legs closed and arms on the sides of the body[1]. However, real exposures involve realistic postures rarely in a fixed standing position. Examples of such real-life postures, include walking, sitting and running, etc. In such postures, radiosensitive organs—gonads, kidneys, spleen and liver—may be exposed to a greater level of radiation than that when the legs are not in a closed and upright position. It is therefore of interest to quantify effects of different postures on the assessed organ equivalent doses and to potentially improve the dose calculations for situations where more accurate dosimetry is desirable. Han *et al*.[2] simulated a worker who walks on contaminated ground using RPI walking phantoms and reported organ equivalent dose difference up to 78 %. Olsher and Van Riper[3] developed a sitting MIRD phantom to simulate scenarios involving a person sitting in ^{60}Co contaminated surroundings and indicated a significantly higher gonad equivalent dose. However, the MIRD phantoms that Olsher *et al*. used have poor anatomical shapes and are difficult to deform.

This paper presents the development of RPI sitting phantoms that represent a pair of adult male and female in the sitting posture. These phantoms are coupled with mesh-based deformation and posture changing software algorithms to automatically adjust the position and posture. Organ and body sizes of these phantoms are compatible with the reference data recommended by the ICRP Publications 23 and 89[4, 5]. This paper also describes applications of these phantoms to two environmental exposure situations involving ^{137}Cs sources on the ground and a PET scanner. To understand the effect of the sitting posture, organ equivalent doses and effective doses from the sitting phantoms are compared with those obtained from upright standing phantoms.

METHODS

In this study, a sitting individual irradiated by radiation sources from below the body was considered. It was hypothesised that, without shielding by the legs, internal organs would be expected to be exposed to a greater level of the radiation. In addition, major organs are closer to the ground than those in a standing posture. To test this hypothesis, two computational sitting phantoms were constructed and incorporated into the MCNPX code for organ dose calculations.

Modelling of sitting phantom

Two new phantoms, RPI sitting phantoms, were constructed from a pair of standing phantoms called RPI-adult male (AM) and RPI-adult female (AF) developed recently by the group here[6]. RPI-AM and AF were designed using data recommended in ICRP Publications 23 and 89[4, 5] for reference adult males and females[4–6]. Based on the polygon mesh

geometry, each phantom consists of more than 140 deformable organs and tissues.

A scalar multiplication method was developed to deform the body surface and organs into the sitting posture[6]. The volume change in the deformed organ mesh models would maintain agreement within 1 % with ICRP recommended reference values. A commercial software package, Rhinoceros, was also used to perform translation, rotation, scaling and fitting of organ models directly in the 3D mesh space.

Figure 1 shows the anatomy of RPI sitting phantoms and RPI-AM and AF, which were used for dose calculation comparison.

The only difference between two sets of phantoms is the position of legs. However, sitting position shortens the distance between torso and ground and exposes the testes, which is supposed to increase the dose.

After the posture adjustments, the mesh-based sitting phantoms were prepared for implementation into the Monte Carlo N-Particle eXtended version (MCNPX) code for organ equivalent dose calculations[7]. Since MCNPX does not handle mesh geometry, a voxelisation software to convert mesh phantoms to voxel phantoms was developed. RPI sitting phantoms were voxelised at resolutions of 2.7 and 2.5 mm, respectively, to keep the total number of voxels to be <25 million—a limit in the MCNPX code. To confirm the anatomical fidelity of the transformed phantoms, the mass and volume of each organ in the voxel domain were checked.

Monte Carlo calculations

To maximise the Monte Carlo computational efficiency, an in-house software was used to create MCNPX input file from a finalised voxel phantom using the standard 'repeated structures' feature of the MCNPX. This feature allowed one to define a space that contains the whole 3D-dimensional array of voxels and then to fill the phantom box with voxels of a different tissue property (assigned to different organs). Organ-specific elemental compositions were based on reference values of the ICRP Publication 89[5].

The MCPLIB04 cross-sectional library for the anatomic interactions based on EPDL 97 evaluation was used[7]. Standard nuclear physics models for photon transport included fluorescence, coherent and incoherent scattering, pair production and bremsstrahlung generation[8]. Electrons were tracked with the integrated tiger series energy indexing. The photon and electron cut-off energies were set to be 0.01 and 0.07 MeV, respectively.

Scenario 1: a person sitting above contaminated ground

Figure 2 shows the ground contamination scenario assuming isotropic planar source of ^{137}Cs (662 keV) under a 2-cm layer of soil with a concentration of 30 kBq m^{-2}. A person sits in the centre of contaminated ground. The square ground area is set to be 30 m × 30 m since Han et al.[2] showed that the effective
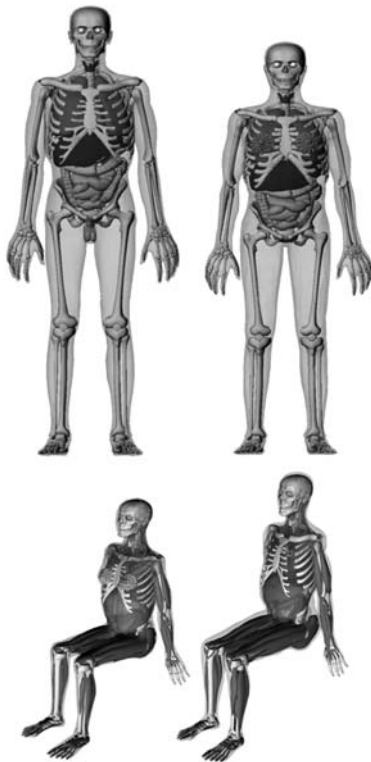

Figure 1. RPI-AM and -AF phantoms (top) and RPI sitting phantoms representing sitting adult male and adult female (bottom).

Figure 2. Ground contamination scenario showing a person in a sitting posture assuming isotropic planar source of ^{137}Cs (662 keV) under a 2-cm layer of soil with a concentration of 30 kBq m^{-2}.

dose difference from 30 m × 30 m and 40 m × 40 m area is < 2 %.

Scenario 2: a person sitting above a PET clinic

Positron emission tomography (PET) is a nuclear medicine imaging method that is gaining popularity. Figure 3 illustrates a scenario where a patient undergoes the PET examination in a PET clinic and a person sits upstairs right above the patient. The administrated ^{18}F-FDG radioactivity is assumed to be 550 MBq according to a protocol used at Massachusetts General Hospital, Boston, MA. After ^{18}F-FDG injection, the patient waits in a room for 60 min to allow for uptake. Then the patient is moved to the imaging room for the 30-min PET scanning. For simplicity, the patient was represented as a point source emitting photons of 511 keV. The distance between the patient and the sitting phantom was 3 m, and the concrete roof had a thickness of 19.5 cm. The half-life of ^{18}F is 110 min. Therefore, during the 30-min examination time, the average activity was 343 MBq or 686 million annihilation photons were emitted isotropically per second. Assuming a full occupying rate for the image room, there were 16 examinations in an 8-h working day.

RESULTS AND DISCUSSION

Table 1 summarises the organ equivalent dose of male sitting and standing phantoms. For both scenarios, 2 billion particles were simulated. The statistical uncertainties for most organ equivalent doses were < 1 %.
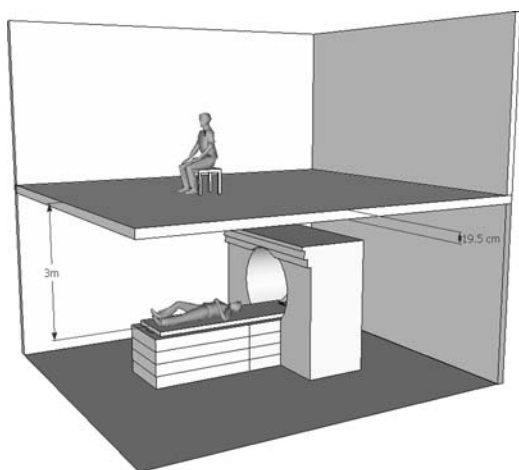

Figure 3. A person sitting upstairs above a PET clinic involving 16 patients a day.

Scenario 1

Organ equivalent dose for the kidney, lungs, red bone marrow, gonads, liver and brain for the sitting phantom are compared with the standing RPI-AM and -AF phantoms. The effective dose for the sitting phantoms was found to be 38.7 nSv h^{-1}, which was 2.3 % more than the standing phantoms. The organ equivalent dose ratios of the sitting and standing phantoms were plotted in Figure 4.

The results show that the largest organ equivalent dose difference lie in male gonads (testes). The sitting posture causes testes to receive 40 % more equivalent dose compared with the standing posture, while the equivalent dose differences of other major organs are within 7 %. Analysis reveals that in isotropic planar source situation, the majority of lateral radiation to the testes is shielded by the thighs of the standing phantom. However, in the sitting posture, the testes are no longer situated between legs but exposed directly to the radiation. In general, the posture change from standing to sitting has two effects: (1) distance between organs and contaminated ground shortens; (2) the bent legs of sitting phantom shield radiation from a relatively large area in front of the phantom compared with the small area right under the phantom in standing posture. Obviously, the first effect increases organ equivalent doses but the second reduces. For the upper organs such as brain and lungs, the first effect dominates;

Table 1. Comparison of organ and effective dose rates (nSv h^{-1}) of male sitting and standing phantoms.

| Organ	Ground (^{137}Cs 30 kBq m^{-2})		PET clinic (F-18 550 MBq)	
	Standing	Sitting	Standing	Sitting
Kidneys	39.77	38.13	144.72	200.00
Lungs	40.16	41.17	123.44	172.86
Lymph nodes	50.08	49.61	358.37	608.74
Muscle	48.30	48.25	331.15	534.95
Oral mucosa	46.76	45.33	135.05	175.91
Slavia glands	47.48	48.43	88.62	126.15
Skin	52.68	53.68	580.57	732.36
Endosteum	58.69	58.99	495.40	665.40
Red bone marrow	39.82	40.01	176.42	302.44
Adrenal	42.73	41.00	184.20	187.06
Gonads	51.24	71.68	555.56	1202.94
Colon	39.99	36.62	186.58	367.71
Stomach wall	35.54	34.54	127.72	202.02
Oesophagus	41.99	43.96	81.97	120.99
Liver	39.46	37.97	176.40	243.27
Thyroid	41.37	36.91	92.79	119.68
Brain	40.67	42.90	76.22	113.93
Bladder wall	42.88	42.14	430.82	736.63
Remainder	45.60	43.63	169.82	254.48
Effective dose	36.86	37.73	182.21	317.38
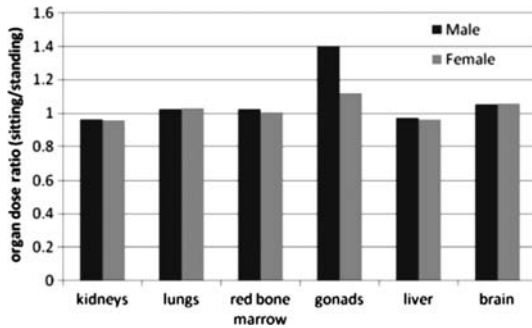
Figure 4. Organ equivalent dose comparison showing dose ratio of standing and sitting phantoms in the environmental exposure scenario involving isotropic planar source under a 2-cm soil with concentration of 30 kBq m^{-2}.
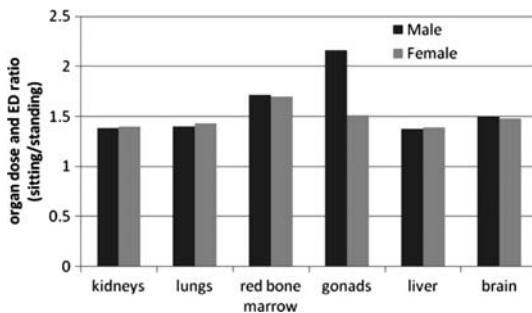

Figure 5. Organ equivalent dose ratio of sitting and standing phantoms in the PET clinic scenario involving 511-keV photons from patients during 8-h working day.

while for the lower organs like kidneys and liver, it is the opposite condition. Therefore, the equivalent doses for brain and lungs increase by 5 and 3 %, respectively, and equivalent doses for kidneys and liver decrease by 4 %. Also, owing to these two competing factors, the increase of effective dose is not significant (2.3 %).

Scenario 2

In the PET clinic scenario, the effective dose of the sitting phantom is 2.54 μSv d^{-1}. The ratios of equivalent doses from the sitting and standing phantoms were plotted in Figure 5 to show the differences of these two postures.

The results show a significant equivalent dose difference (up to 117 % for the male testes) to nearly all the organs between the walking and standing phantoms. The effective dose difference is 57 %, respectively, for the male and female phantom. The reason for such discrepancies is the point source and inverse square law. The position change from

standing to sitting made the phantom around 0.5 m closer to the point source, which causes 40 % higher exposure. Additional shielding by the closed legs also contributed to some of the discrepancies involving the testes.

DISCUSSION

Results clearly show that, in the sitting posture where the legs no longer shield certain organs from radiation below the feet, several organs especially including the male gonads (testes) will receive additional exposures. Similar situation occurs in the crouching and squatting postures. Meanwhile, it should also be noted that the results above are based on the assumption of isotropic planar source for ground contamination. Han et al.[2] found that, if a parallel beam source was used, the equivalent dose discrepancy for testes should be less significant; however, the equivalent dose discrepancies for other internal organs such as liver and kidney are supposed to be more significant. The form of source as well as the specific human posture is important parameters that will determine the dose level in practical exposure scenarios. It is therefore prudent to consider the body shielding effects for radiosensitive organs (such as the testes) in situations where certain postures are involved. Such an approach may be necessary when performing dose reconstruction for high-dose exposure.

CONCLUSIONS

This study developed a pair of sitting phantoms and evaluated the effect of the sitting posture on environmental dose assessment. The MCNPX code was used to perform the dose calculations for two exposure scenarios. In the ground contamination scenario, organ equivalent doses from isotropic planar sources of ^{137}Cs with a contamination concentration of 30 kBq m^{-2} showed no significant difference to most organs, except for male testes (40 % increase). In the scenario, in which a 511 keV photon point source is used, the effective dose for male sitting phantom is 2.54 μSv d^{-1} (8-h working day). Most organ equivalent doses of sitting phantoms are found to increase by 40–117 % when compared with those from the standing phantoms. Such increase in assessed dose comes from the reduced distance between the sitting phantoms and source. The study demonstrated that deformable phantoms with realistic postures such as sitting are potentially useful in improving organ equivalent dose calculations in certain environmental dosimetry studies requiring greater accuracy.

REFERENCES

1. Xu, X. G. *Chapter 1. Computational phantoms for radiation dosimetry: a 40-year history of evolution*. In: Handbook of Anatomical Models for Radiation Dosimetry. Xu, X. George and Eckerman, Keith F., Eds. Taylor & Francis (2009).

2. Han, B., Zhang, J., Na, Y., Caracappa, P. and Xu, X. G. *Modeling and Monte Carlo organ dose calculations for workers walking on ground contaminated with Cs-137 and Co-60 gamma sources*. Radiat. Prot. Dosim. **141**(3), 299–304 (2010).

3. Olsher, R. and Van Riper, K. *Application of a sitting MIRD phantom for effective dose calculations*. Radiat. Prot. Dosim. **116**(1–4), 392–395 (2005).

4. International Commission on Radiological Protection. *Report of the task group on Reference Man*. ICRP Publication 23. Pergamon Press (1975).

5. International Commission on Radiological Protection. *Basic anatomical and physiological data for use in radiological protection: reference values*. ICRP Publication 89. Pergamon Press (2002).

6. Zhang, J., Na, Y., Caracappa, F. P. and Xu, X. G. *RPI-AM and RPI-AF, a pair of mesh-based, size-adjustable adult male and female computational phantoms using ICRP-89 parameters and their calculations for organ doses from monoenergetic photon beams*. Phys. Med. Biol. **54**, 5885–5908 (2009).

7. White, M. C. *Photoatomic data library MCPLIB04: a new photoatomic library based on data from ENDF/B-VI Release 8*. Los Alamos National Laboratory internal memorandum X-5:MCW-02-111. Los Alamos National Laboratory (2002).

8. *MCNPX User's Manual, Version 2.5.0*. Los Alamos National Laboratory. Report No. LA-UR-02-2607. Los Alamos National Laboratory (2005).